

# Modulation of Cholesterol Homeostasis by Antiproliferative Drugs in Human Pterygium Fibroblasts

Enrico Peiretti,<sup>1</sup> Sandra Dessì,<sup>2</sup> Claudia Mulas,<sup>2</sup> Claudia Abete,<sup>2</sup> Claudia Norfo,<sup>2</sup> Marirosa Putzolu,<sup>2</sup> and Maurizio Fossarello<sup>1</sup>

**PURPOSE.** The authors have previously shown that the growth of cultured fibroblasts obtained from primary pterygia was associated with an increase in cholesterol esterification, suggesting that alterations of cholesterol homeostasis may be involved in the development and progression of this disorder. This investigation was conducted to determine whether antiproliferative agents such as pioglitazone (PIO) and everolimus (EVE) may inhibit proteins involved in the cholesterol ester cycle and the proliferation of pterygium fibroblasts (PF).

**METHODS.** Quiescent normal conjunctival fibroblasts and PFs were treated with or without inhibitors of cell proliferation (PIO and EVE) or with inhibitors of cholesterol esterification—progesterone (Pg) and Sandoz compound (SaH)—and then were stimulated to growth by 10% fetal calf serum (FCS). Cell proliferation was assessed by counting cells. Trypan blue uptake was used to determine cell viability. mRNA and protein levels were determined by reverse transcription-polymerase chain reaction (RT-PCR) and Western blot analysis, respectively.

**RESULTS.** PIO and EVE significantly abolished the increase in cholesterol esters, acyl-coenzyme A cholesterol acyltransferase (ACAT1), and multidrug resistance protein (MDR1) mRNA observed in growing cells. Each inhibitor upregulated ATP-binding cassette-A1 (ABCA1), neutral cholesterol ester hydrolase (NCEH) mRNA, and caveolin-1 expression in a manner similar to that of specific inhibitors of cholesterol esterification such as Pg and SaH.

**CONCLUSIONS.** Intracellular modifications of cholesterol homeostasis may be relevant to pterygium development. Moreover, antiproliferative agents such as PIO and EVE may represent a potential topical medication in the prevention and inhibition of pterygium growth at an early stage, probably by modulation of cholesterol ester metabolism. (*Invest Ophthalmol Vis Sci.* 2007;48:3450–3458) DOI:10.1167/iovs.06-1054

Pterygium is a common proliferative disorder involving epithelial hyperplasia and fibrovascular proliferation. In the advanced stages, pterygium can necessitate complex surgery

for full visual rehabilitation and recurrences, and ocular complications are not infrequent.<sup>1–6</sup> Ultraviolet (UV) light has long been associated as the etiologic agent of pterygium,<sup>7–9</sup> and recently heparin-binding epidermal growth factor (HB-EGF), a potent mitogen, was localized in pterygium tissue and was demonstrated to be significantly induced by UVB in pterygium-derived epithelial cells.<sup>10</sup> In populations with high exposure to ultraviolet radiation, including our region (Sardinia, Italy), the rate of occurrence is high and represents an important cost for the national healthcare.<sup>11</sup>

Although the pathogenesis of pterygium is yet undetermined, tumorlike histologic characteristics, ranging from mild dysplasia to carcinoma in situ and local invasiveness, have been described by different authors.<sup>12–14</sup> Moreover, pterygium fibroblasts (PFs) exhibit characteristics of the transformed phenotype,<sup>15</sup> microsatellite instability, and loss of heterozygosity,<sup>16</sup> all reported to be common findings in neoplastic tissue.

Recently, our laboratory has identified that alterations in cholesterol metabolism,<sup>17</sup> mainly in cholesterol esterification, occur during the growth of fibroblasts isolated from human pterygia. These results prompted us to question whether key molecules involved in the regulation of intracellular cholesterol homeostasis may participate in the proliferative phase of this disease. Those molecules include acyl-coenzyme A cholesterol acyltransferase (ACAT1), which is the enzyme responsible for intracellular cholesterol ester formation; multidrug resistance protein (MDR1), which has been implicated in cholesterol transport from the plasma membrane to the endoplasmic reticulum (ER); caveolin-1, the key structural protein of caveolae, a suggested possible carrier of excess cholesterol from the ER to the caveolae-plasma membrane; neutral cholesterol ester hydrolase (nCEH), the enzyme responsible for the hydrolysis of cholesterol esters; and ATP-binding cassette-A1 (ABCA1), the protein that mediates cholesterol efflux. Relevant ACAT1 and MDR1 are induced, and nCEH, ABCA1, and caveolin-1 are depressed during the growth of several types of tumor cells.<sup>18–22</sup>

Given the results of our previous investigations, the present study was designed to explore whether altered expression of these proteins may be important for fibroblast growth stimulation, which represents an essential phase for pterygium progression and recurrence. We evaluated the effect of everolimus (EVE) and pioglitazone (PIO) on the expression of proteins involved in the cholesterol ester cycle in fibroblasts isolated from pterygium and stimulated to grow with 10% fetal calf serum (FCS). PIO, an insulin-sensitizing agent, and EVE, an immunosuppressive agent, are novel drugs that have been developed for the treatment of insulin resistance and for the prophylaxis of transplant rejection, respectively.<sup>23,24</sup> These agents may have clinical benefits in proliferative diseases because both have significant in vitro and in vivo antiproliferative activity against a broad range of human cell lines. In the same cells, we also evaluated the effect of two well-known cholesterol esterification inhibitors, progesterone (Pg) and the acyl amide ACAT inhibitor Sandoz compound 58–035 (SaH).

From the <sup>1</sup>Department of Surgical Sciences, Eye Clinic, and the <sup>2</sup>Department of Science and Biomedical Technologies, Experimental Pathology Section, University of Cagliari, Cagliari, Italy.

Presented at the annual meeting of the Association for Research in Vision and Ophthalmology, Fort Lauderdale, Florida, April 2005.

Supported by grants from “Ministero dell’Università e Ricerca Scientifica” (and “ex 60%”) and “Regione Autonoma della Sardegna.”

Submitted for publication September 6, 2006; revised December 4, 2006, and January 16, 2007; accepted May 21, 2007.

Disclosure: E. Peiretti, None; S. Dessì, None; C. Mulas, None; C. Abete, None; C. Norfo, None; M. Putzolu, None; M. Fossarello, None

The publication costs of this article were defrayed in part by page charge payment. This article must therefore be marked “advertisement” in accordance with 18 U.S.C. §1734 solely to indicate this fact.

Corresponding author: Maurizio Fossarello, Department of Surgical Sciences, Eye Clinic, University of Cagliari, Via Ospedale, I-09124 Cagliari, Italy; mfossarello@libero.it.

## PATIENTS, MATERIALS, AND METHODS

### Patient Selection

We recruited six patients with primary pterygium (age range, 45–65 years; mean,  $57.33 \pm 3.5$  [SE] years) and six patients with normal conjunctiva (age range, 60–70 years; mean,  $63.66 \pm 1.45$  years), who underwent cataract surgery at the University Eye Clinic of Cagliari. Diagnosis of pterygium was based on clinical history and evaluation of signs and symptoms. All patients with pterygium (three men and three women) had at least a 3-year history of a slow-growing lesion, with a corneal extension of at least 4 mm, as measured with a caliper, from the limbus to the corneal vertex. Pterygia morphology was clinically graded according to the system of Tan et al.,<sup>25</sup> based on the assessment of pterygium translucency: atrophic (T1), intermediate (T2), or fleshy (T3) pterygium. All pterygia collected in this study were T3. The control group (normal conjunctiva) included three men and three women undergoing surgery for cataract extraction. No subject in the control group had any inflammatory signs or symptoms. The research adhered to the tenets of the Declaration of Helsinki. Written informed consent was obtained from all the patients before tissues were collected. This study and all the procedures, including biopsy from the conjunctiva during cataract surgery, were approved by the Ethics Committee of the University of Cagliari.

All tissue samples were obtained as previously described.<sup>17</sup> In summary, at the time of surgery, tissue was excised from the inner canthus with microforceps. As a rule, within 1 hour of excision, samples were placed in sterile boxes containing a preservative solution (Eurocollins; Roche Biochemicals, Mannheim, Germany) and were transferred to the cell culture room.

### Fibroblast Isolation

For fibroblast isolation, pterygium and normal conjunctiva tissues were dissected into three to four tissue fragments ( $1 \text{ mm}^2$ ). Tissue fragments were placed in six-well plates for 2 hours. After 2 hours of adhesion, a few drops of Dulbecco modified Eagle medium (DMEM; Gibco, Grand Island, NY) supplemented with 10% fetal bovine serum (FBS; Sigma Aldrich, Munich, Germany), 100 U/mL penicillin/streptomycin (Sigma Aldrich), and fungizone (Life Technologies, Bethesda, MD) were added to cover each fragment. The next day, the tissue fragments were covered with culture medium and were placed in a humidified incubator ( $37^\circ\text{C}$ , 5%  $\text{CO}_2$ ). The medium was changed every 2 days. After 5 to 6 days, fibroblasts began to proliferate from the fragment margin (halo of cells) and created a monolayer. The outgrowing cells were morphologically consistent with fibroblasts by their characteristic spindle shape. After 4 weeks, fibroblasts were purified by repeat trypsinization (trypsin/EDTA, 0.05%/0.02%) and passaging to achieve a homogeneous population of spindle cells. Purified fibroblasts were washed twice with sterile phosphate-buffered saline (PBS) and centrifuged. Cells ( $1 \times 10^6$ ) were then seeded into a  $25\text{-cm}^2$  culture flask and grown to confluence. At this time, cells were used for *in vitro* staining experiments or were transferred to cryopreservation medium at a suspension of  $1 \times 10^7$  cells/mL. After swift freezing, fibroblasts were placed in liquid nitrogen for long-term storage. Based on the need of experiments, cryopreserved cells were removed from liquid nitrogen tank and cultured under the conditions described. All experiments were conducted using fibroblasts between passages 2 to 4.

For *in vitro* kinetic experiments, cells were placed at a density of 10,000 cell/ $\text{cm}^2$  in six-well plates and then were incubated for 48 hours in DMEM with 0.2% FCS to synchronize cells at a quiescent state. Quiescent fibroblasts were then diluted in complete growth medium with 10% FCS, supplemented or not with 50  $\mu\text{M}$  PIO (supplied by Takeda Chemical Industries, Ltd., Osaka, Japan) or 20 nM EVE (supplied by Novartis Pharma AG, Basel, Switzerland). In addition, 10  $\mu\text{M}$  P<sub>g</sub> (Sigma-Aldrich, St. Louis, MO) and 4  $\mu\text{M}$  acyl amide ACAT inhibitor SaH (Novartis Pharma AG) were added to some cells as a broad-spectrum regulator of the cholesterol ester cycle. Preliminary experiments were carried out to evaluate the doses of drugs exerting minor effects on cell viability. Cells were harvested at indicated time points

after treatment. Cell proliferation was assessed by counting cells with a hemocytometer. Trypan blue uptake was used to determine cell viability.

### Cellular Neutral Lipid Staining

To determine whether abnormal cell growth is associated with alterations in intracellular lipid metabolism, we determined intracellular lipid deposits in primary culture of PFs and normal conjunctival fibroblasts (NCFs). After isolation from ocular tissues, the fibroblasts were cultured in a tissue culture chamber, as described. After the indicated time of incubation, the cells were washed three times with PBS and fixed by soaking in 10% formalin. The cells were treated with isopropyl alcohol (60%) and washed, and nuclei and intracellular neutral lipid droplets were then stained with Mayer hematoxylin solution (Sigma Aldrich, Munich) and oil red O, respectively. Stained cells were examined by light microscopy. The color intensity of the red, indicating neutral lipid accumulation in each cell, was quantified with the National Institutes of Health Image 1.63 Analysis Software program (Scion Image).

### RT-PCR Analysis

Expression levels of ACAT1, MDR1, nCEH, and ABCA1 mRNAs were evaluated in PFs and in NCFs by semiquantitative, reverse transcription polymerase chain reaction (RT-PCR) with  $\beta$ -actin as RNA controls. Approximately  $10^6$  cells were untreated or treated with the drugs. RNA extractions were performed using reagent (Trizol; Invitrogen).

Equal amounts of total RNA (1  $\mu\text{g}$ ) were reverse transcribed into cDNA using the random hexamer method. cDNA was subsequently amplified by PCR in the presence of specific primers according to the instructions provided by the manufacturer (GeneAmp RNA PCR Kit; Perkin-Elmer Cetus, Foster City, CA).

PCR was performed using the following primers and conditions: for ACAT1, 5'AGCAGAGGCAGAGGAATTGA3', 5'GCACACCTGGCAAGATGAG 3' (466-bp fragment),  $95^\circ\text{C}$  for 30 seconds,  $58^\circ\text{C}$  for 50 seconds, and  $72^\circ\text{C}$  for 60 seconds for 40 cycles; for MDR1, 5'CCCATCATTGCAATAGCAGG3', 5'GTTCAAACITCTGCTCCTGA3' (167-bp fragment),  $94^\circ\text{C}$  for 30 seconds,  $55^\circ\text{C}$  for 60 seconds, and  $72^\circ\text{C}$  for 60 seconds for 30 cycles; for nCEH, 5'CTTGTAACCTTGAGTTGGAG3', 5'GTAGGAAGTAACCA-CATTCA3' (151-bp fragment),  $94^\circ\text{C}$  for 30 seconds,  $55^\circ\text{C}$  for 60 seconds, and  $72^\circ\text{C}$  for 60 seconds, for 30 cycles; for ABCA1, 5'TCCTCTCCAGAGCAAAAAGC3', 5'CTCCACAACACTTCACATGGT3' (286-bp fragment),  $95^\circ\text{C}$  for 30 seconds,  $62^\circ\text{C}$  for 60 seconds, and  $72^\circ\text{C}$  for 30 seconds, for 30 cycles; for  $\beta$ -actin, 5'AGGGGCCGGACTCGTCATACT 3', 5'GGCGGCAC-CACCATGTACCCT 3' (202-bp fragment);  $96^\circ\text{C}$  for 30 seconds,  $60^\circ\text{C}$  for 59 seconds, and  $72^\circ\text{C}$  for 45 seconds, for 20 cycles.

Subsaturation levels of cDNA templates needed to produce a dose-dependent amount of PCR product were defined in initial experiments by testing a range of template concentrations. Subsequent PCR was carried out with subsaturation levels of RT reactions with identical amplification parameters.

### Blotting Analysis

During PCR reaction the nonradioactive label, digoxigenin-11-dUTP (DIG; Boehringer Mannheim, Mannheim, Germany) was incorporated and immunodetected with anti-digoxigenin Fab fragments conjugated to alkaline phosphatase and was visualized with a chemiluminescence substrate (CSPD; Applied Biosystems, Foster City, CA). Enzymatic dephosphorylation of the chemiluminescence substrate (CSPD; Applied Biosystems) by alkaline phosphatase led to light emission at a maximum wavelength of 477 nm that was recorded on x-ray films. DNA fragments were separated by electrophoresis on agarose and then blotted onto a nylon membrane for 16 h in  $10\times$  SSC. The blot was exposed to x-ray film for 2 to 10 minutes. An image analysis system (Digital Science Band Scanner; Eastman Kodak, Rochester, NY) containing image analysis software (ScanJet ID Image Analysis Software; Hewlett-Packard, Palo Alto, CA) was used to assess the intensity of the bands in the autoradiograms.

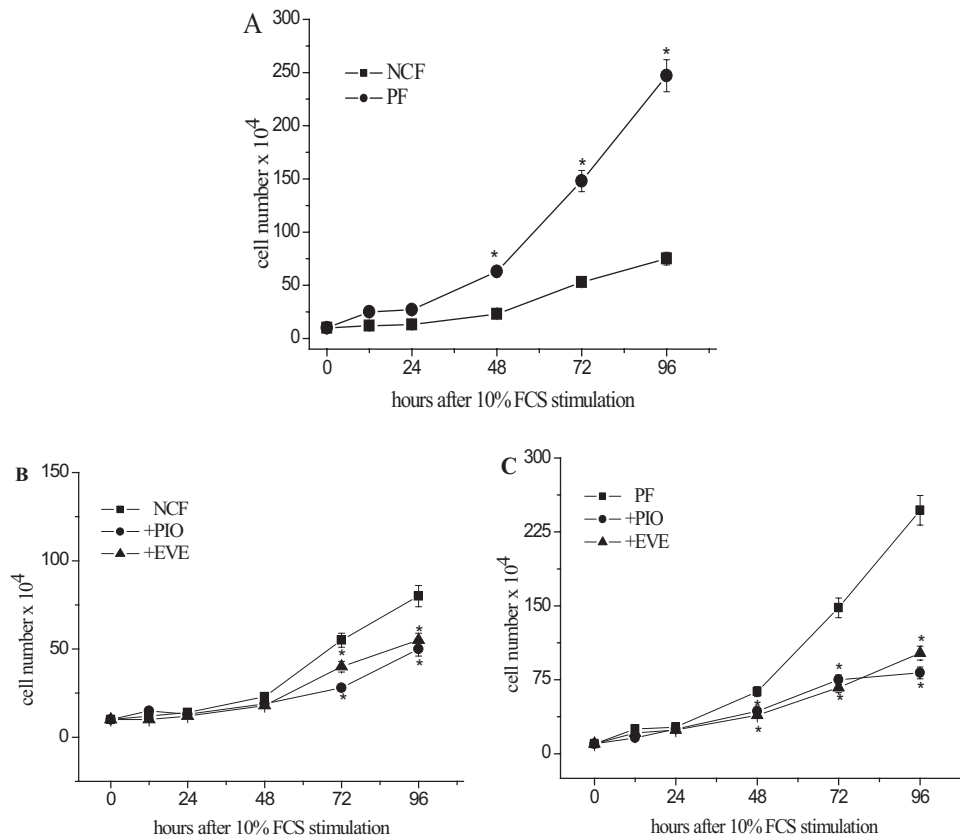


**FIGURE 1.** PIO and EVE inhibit cell growth. NCFs and PFs were stimulated with 10% FCS in the absence (A) or in the presence of either PIO (50  $\mu$ M; B) or EVE (20 nM; C) and were harvested 24, 48, 72, or 96 hours later. Results are mean  $\pm$  SE of NCF and PF cultures from six patients and six controls. \* $P < 0.05$ .

The overall procedure was standardized by expressing the amount of PCR product for each target mRNA relative to the amount of product formed for  $\beta$ -actin. Because a low yield of PCR products is often obtained when cDNA segments are coamplified with an internal standard gene in the same tube, the relative levels of gene expression were determined by comparing the PCR products of the target cDNA and the  $\beta$ -actin gene processed in separate tubes.

### Preparation of Protein Samples and Western Blot Analysis

Cell lysates were prepared with lysis buffer (10% SDS in 50  $\mu$ M Tris, 1  $\mu$ M EDTA [pH 7.5], 50  $\mu$ M dithiothreitol [DTT], and protease inhibitor cocktail [Sigma]), incubated at 37°C and sheared with a syringe fitted with an 18-gauge needle to homogeneity. Protein concentrations of the cell lysates were determined using a modified Bradford protein assay (Bio-Rad Laboratories, Hemel Hempstead, UK). Protein samples (30  $\mu$ g) were then subjected to 12% sodium dodecyl sulfate-polyacrylamide gel electrophoresis (SDS-PAGE). After gel separation, the proteins were transferred to a polyvinylidene difluoride (PVDF) membrane (Invitrogen). The membrane was blocked with 5% milk in TBST (50  $\mu$ M Tris-HCl, pH 7.6, 0.15 M NaCl, and 0.05% Tween-20) at room temperature for 1.5 hours and was incubated with affinity-purified rabbit anti-ACAT1 antibody H-125 and anti-caveolin-1 (Santa Cruz Biotechnology, Santa Cruz, CA) in 5% milk-TBST at room temperature for 1.5 hours and with HRP-conjugated anti-rabbit secondary antibody (Santa Cruz Biotechnology) for an additional 1.5 hours. After incubation, the membrane was washed extensively with TBST. The immunoreactive band was visualized by using enhanced chemiluminescence (ECL) detection reagent (Amersham, Uppsala, Sweden).

### Statistical Analysis

Mean  $\pm$  SE for triplicate determinations are presented. Student's *t*-test was used to determine statistical significance of differences. For all statistical analyses, the level of significance was set at  $P < 0.05$ .

## RESULTS

### Effects of PIO and EVE on Proliferation and Neutral Lipid Accumulation in Fibroblasts Derived from Pterygium

Growth stimulation with 10% FCS resulted in a significant increase in cell numbers of PF compared with NCF (Fig. 1A;  $P < 0.05$ ). As expected, PIO and EVE treatments resulted in a dramatic suppression of cell growth in NCFs and PFs. However, this effect was more prominent in PFs than in NCFs (Figs. 1B, 1C;  $P < 0.05$ ).

We next determined the cytoplasmic neutral lipid accumulation in NCFs and PFs by directly staining cytoplasmic neutral lipid droplets with oil red O. As shown in Figures 2A and 2B, unstimulated PFs accumulated more neutral lipids droplets than NCFs (Fig. 2A, time 0). When cells were growth stimulated with 10% FCS, the cytoplasmic staining became more apparent in NCFs and PFs (Figs. 2A, 2B). However, the extent of lipid accumulation in response to FCS was more evident in PFs than in NCFs at all time points considered.

Surprisingly, growth inhibition induced by PIO and EVE was also associated with lack of cholesterol ester accumulation in PFs. Interestingly, this effect was similar to that observed using specific inhibitors of cholesterol esterification, such as Pg and SaH (Figs. 2A, 2C).

### RNA Levels of Protein Involved in Cholesterol Ester Cycle during the Growth of NCF and PF

To determine whether fibroblast growth was associated with modifications of gene expression involved in the cholesterol cell cycle, quiescent NCFs and PFs were stimulated to grow with 10% FCS. As shown in Figures 3A and 3B, ACAT1 and MDR1 mRNA levels significantly increased 24 hours after stimulation in NCFs and PFs. However, the levels of gene



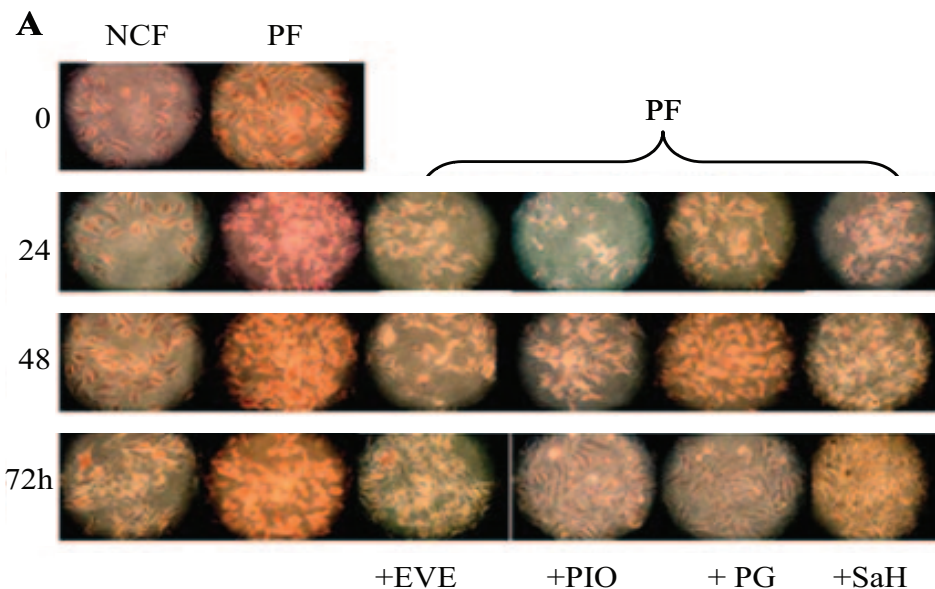
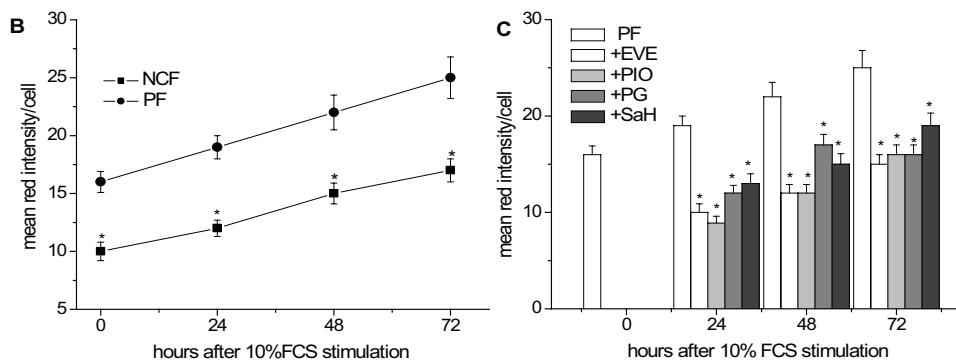


**FIGURE 2.** Lipid droplets in PIO-, EVE-, Pg-, and SaH-treated PF cultures. NCFs and PFs were stimulated with 10% FCS and were harvested 24, 48, or 72 hours later. PFs were also cultured in the presence of PIO (50  $\mu$ M), EVE (20 nM), Pg (10  $\mu$ M), or SaH (4  $\mu$ M). Cells were then fixed and stained with oil red O for neutral lipids. (A) Representative images of oil red O-stained NCF and PF cultures. Graphs show mean red intensity per cell of untreated NCFs and PFs (B) and drug-treated PFs (C), as measured by NIH Image 1.63 Analysis Software (Scion Image). Results are mean  $\pm$  SE of NCF and PF cultures from six patients and six controls. \* $P < 0.05$



expression were significantly higher in PFs than in NCFs at all time points considered. By contrast, nCEH and ABCA1 were lower in PFs than in NCFs (Figs. 3C, 3D). Adding PIO and EVE to culture PFs reduced the mRNA levels of ACAT1 and MDR1 but increased those of ABCA1 and nCEH (Figs. 4A-D, respectively).

**Effect of PIO, EVE, Pg, and SaH on the Expression of ACAT1 and Caveolin1 in Stimulated PFs**

Recently, more reports have confirmed that many proteins involved in the signal cascade are located in lipid rafts/caveolae.<sup>26,27</sup> Maintaining cholesterol levels is essential for functional caveolae and depends, in part, on the interaction of cholesterol with caveolin-1, a major caveolae component. Given the role of signal transducing proteins in cell growth and mitogenesis, we also determined the effect in PFs of PIO, EVE, Pg, and SaH on caveolin-1 protein expression, and we compared it with that of ACAT1 expression. When PFs were exposed to 10% FCS, we observed an increase in ACAT1 protein; by contrast, caveolin-1 strongly decreased (Figs. 5A, 5B). Furthermore, adding cholesterol ester inhibitors (Pg and SaH) and cell proliferation inhibitors (PIO and EVE) significantly suppressed ACAT1 protein expression but significantly increased caveolin-1 expression (Figs. 6A, 6B).

**DISCUSSION**

Pterygium had been considered a chronic degenerative condition but is now thought to be UV light-related uncontrolled

cell proliferation originating from altered limbal epithelial stem cells,<sup>28</sup> with limited local invasion and inability to develop metastases. At the same time, features of the behavior of pterygium suggest excessive or disordered growth (i.e., tumor-like properties).<sup>12-14</sup> Although mechanisms involved in the pathogenesis of pterygia remain largely elusive, several data suggest the existence of intrinsic abnormalities in the pterygial fibrovascular tissue. Pterygium recurs aggressively after surgical excision, and treatment modalities mimic treatments for neoplastic tissue, such as wide excision, adjunctive radiotherapy, and antimetabolic chemotherapy.<sup>1</sup> In recent years, several studies have focused on genetic mutations and epigenetic changes occurring in pterygia. These alterations are similar to those observed in several types of cancer, in which there is damage to cellular regulation and control of the cell cycle. Controversial data have been accumulated on the role of the p53 tumor antigen, which is found in increased amounts in a wide variety of transformed cells: although Dushku and Reid,<sup>29</sup> Tan et al.,<sup>30</sup> and Weinstein et al.<sup>31</sup> reported high expression of p53 in the epithelium overlying the pterygium and Tsai et al.<sup>32</sup> found mutations in the p53 gene in 15.7% of pterygia, other investigators have failed to detect increased p53 protein levels or p53 mutations in pterygia.<sup>33,34</sup> Inactivation by hypermethylation of the promoter of the p16 tumor-suppressor gene and loss of its protein expression has been detected in 16.3% of pterygia,<sup>35</sup> probably resulting in abnormal regulation of the cell cycle. Aberrant methylation of the p16 gene promoter and resultant gene silencing play important roles in the pathogenesis of many types of human cancers.<sup>36</sup>

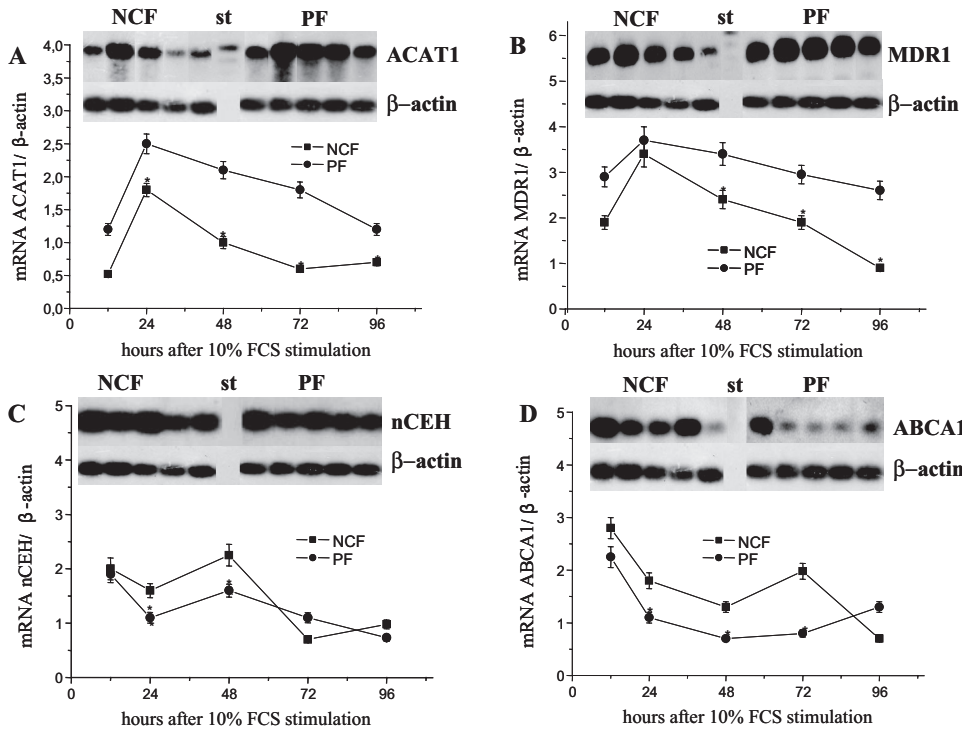


FIGURE 3. mRNA levels of protein involved in cholesterol ester cycle during the growth of NCF and PF. NCFs and PFs were stimulated with 10% FCS and were harvested 24, 48, 72, or 96 hours later. Total RNA was then extracted and analyzed by RT-PCR. (A-D) Representative blot analysis of ACAT-1, MDR1, nCEH, ABCA1, and  $\beta$ -actin mRNAs are shown in the upper part of each. Graphs represent the densitometric values  $\pm$  SE relative to  $\beta$ -actin of NCF and PF cultures from six patients and six controls. \* $P < 0.05$ .

Oncogenic human papillomaviruses (HPVs), notably types 16 and 18, which have been found in pterygia and limbal tumors<sup>37,38</sup> (particularly in certain geographic areas, such as Sardinia, Italy<sup>39</sup>), can disrupt the p53-dependent programmed cell death pathway<sup>40</sup> and assume a potential oncogenic role,<sup>41</sup> eventually interacting with UV irradiation.<sup>42</sup>

Several potent fibrogenic and angiogenic growth factors, such as basic fibroblast growth factor (bFGF), platelet-derived

growth factor (PDGF)-BB, and transforming growth factor (TGF)- $\beta$ 1, have been found by immunohistochemistry in pterygium tissues.<sup>43</sup> Indeed, pterygium head fibroblasts were shown to overexpress matrix metalloproteinase (MMP)-1 and MMP-3 and tissue inhibitor of metalloproteinase (TIMP)-1 and TIMP-2 in culture mediated through the activation of the extracellular regulated kinase (ERK)1/2 mitogen-activated protein kinase (MAPK)-dependent pathway, which is a major regulator of

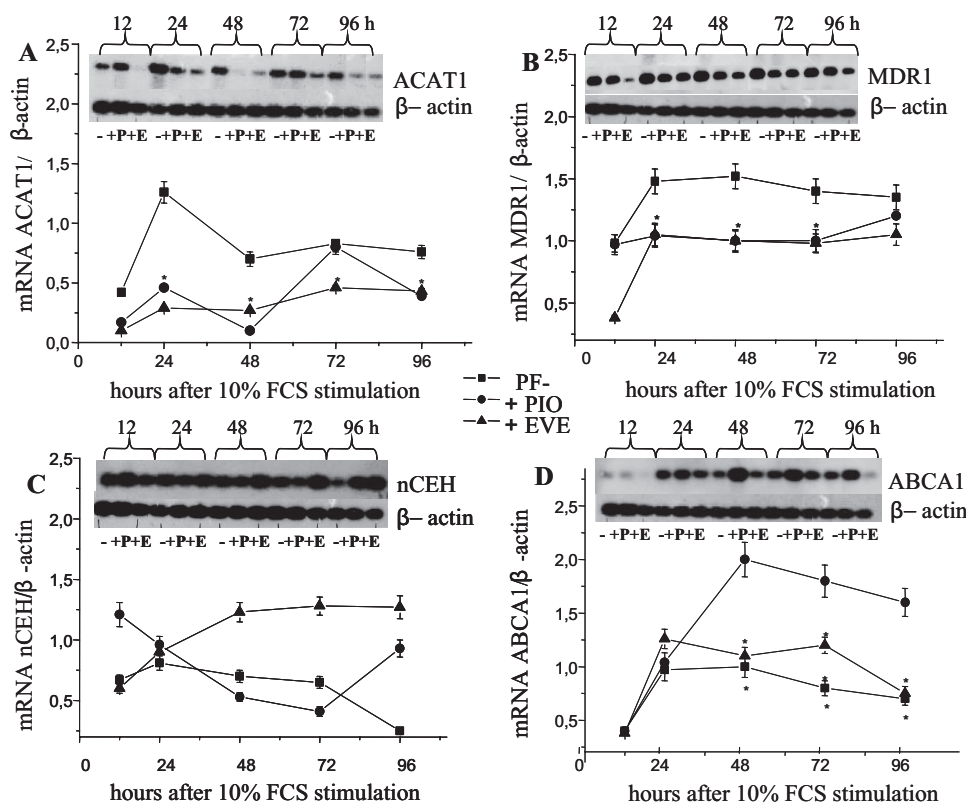
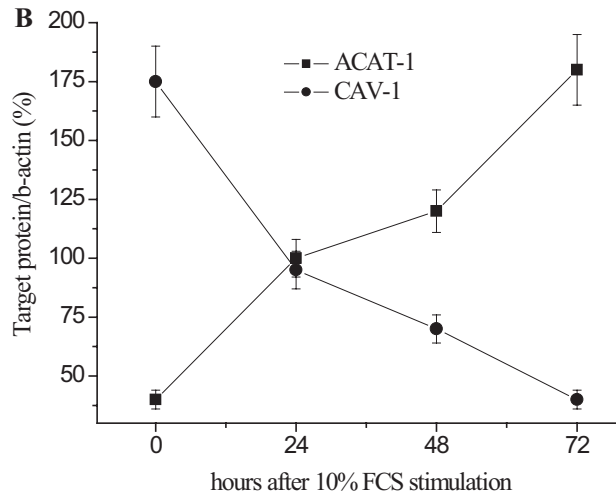
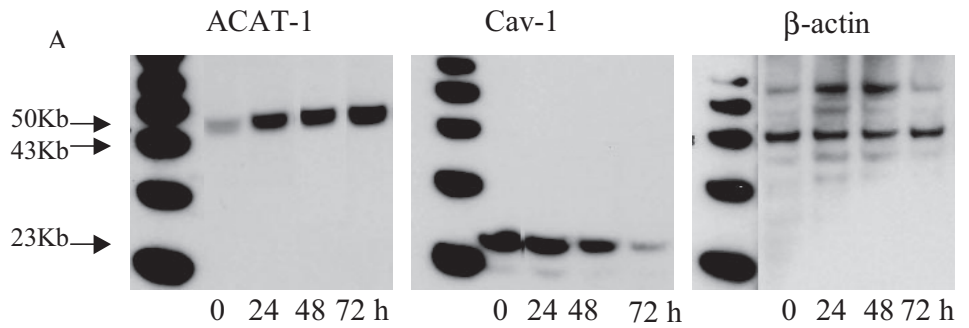
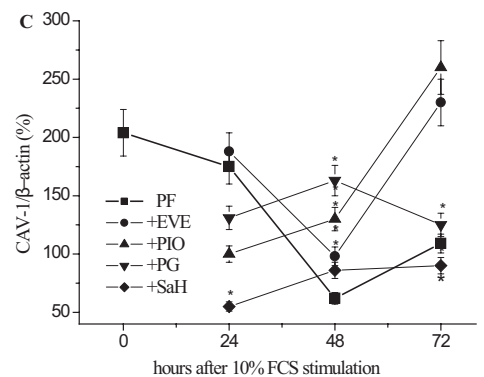
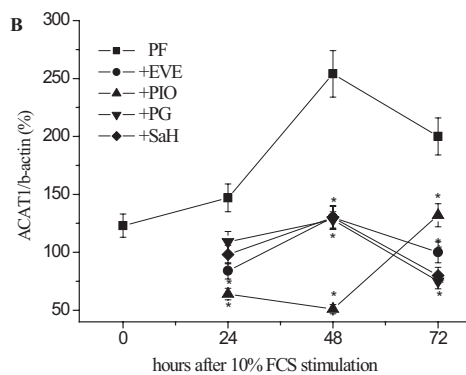
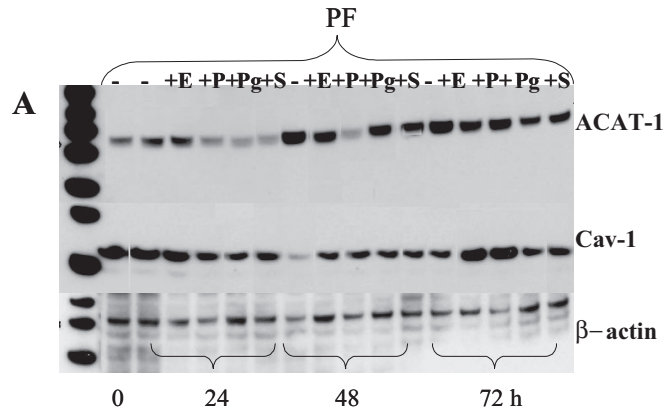


FIGURE 4. Effect of PIO and EVE on mRNA levels of protein involved in cholesterol ester cycle during the growth of PFs. PFs were stimulated with 10% FCS and were harvested 12, 24, 48, 72, or 96 hours later. Total RNA was then extracted and analyzed by RT-PCR. (A-D) Representative blot analysis of ACAT-1, MDR1, nCEH, ABCA1, and  $\beta$ -actin mRNAs are shown in the upper part of each. Graphs represent the densitometric values  $\pm$  SE relative to  $\beta$ -actin of untreated or PIO and EVE treated PF cultures from six patients and six controls. \* $P < 0.05$ .



**FIGURE 5.** Expression of ACAT1 and caveolin-1 protein in growth-stimulated PFs. PFs were stimulated with 10% FCS and harvested 12, 24, 48, or 72 hours later. Proteins were then extracted and subjected to Western blot analysis. (A) Representative blot analysis of ACAT1, CAV-1, and  $\beta$ -actin protein expression. (B) Graph represents the densitometric values  $\pm$  SE relative to  $\beta$ -actin of PF cultures from six patients and six controls.



**FIGURE 6.** Effect of PIO, EVE, Pg, and SaH on the expression of ACAT1 and caveolin-1 protein in growth-stimulated PFs. PFs were stimulated with 10% FCS and harvested 12, 24, 48, or 72 hours later. Proteins were then extracted and subjected to Western blot analysis. (A) Representative blot analysis of ACAT1, CAV-1, and  $\beta$ -actin protein expression. (B, C) Graphs represent the densitometric values  $\pm$  SE relative to  $\beta$ -actin of PF cultures from six patients and six controls. \*Statistically significant differences ( $P < 0.05$ ) versus untreated PFs.

melanoma cell proliferation.<sup>44-50</sup> Given this, it was interesting to note the finding of conjunctival melanocytic pigmented lesions within pterygium.<sup>51</sup>

Microarray analysis studies revealed that mRNA levels of a number of genes related to cell growth, transformation, and tumorigenesis are changed in primary pterygium.<sup>52-55</sup> In particular, increased expression of IGFBP-2 and decreased expression of IGFBP3 have been observed, each of which is correlated with the presence of cancer.<sup>52,55</sup> Moreover, modifications in cholesterol synthesis and metabolism are common findings in neoplastic tissue. We have previously demonstrated that the rate of cell proliferation correlates positively with cholesterol esterification and with ACAT1 and MDR1 mRNA levels in various types of human cell lines.<sup>20-22</sup> We suggested that cholesterol esterification may have a role in regulating the rate of cell growth and division and that MDR1 may contribute to this regulation by modulating the availability of cholesterol substrate in the ER, which, in turn, is a major determinant of ACAT activity.<sup>56</sup> We also presented evidence that freshly isolated PFs contain higher levels of cholesterol esters than fibroblasts from normal conjunctiva and that they respond to mitogenic stimuli by significantly increasing cellular lipid content above constitutive levels.<sup>17</sup> These results provide support for the concept that the presence of high levels of intracellular cholesterol esters could represent a cell phenotype predisposing to the development of pterygial lesions.

In the present study, we used an in vitro system with fibroblasts derived from human pterygia to evaluate whether antiproliferative agents able to modulate the cholesterol esterification may eventually interfere with their growth. Administration of PIO and EVE was effective at inhibiting PF growth, combined with a significant abolition of the increase in cholesterol esters, in ACAT1, and MDR1 mRNA, which are usually observed in abnormally growing cells.<sup>20,21</sup> Both inhibitors upregulated ABCA1 and NCEH mRNA and caveolin-1 expression in a manner similar to that for specific inhibitors of cholesterol esterification, such as Pg and SaH compound.

PIO and an analog of EVE inhibit corneal and choroidal neovascularization in animal models.<sup>57-59</sup> It has been suggested that this effect probably results from their recognized anti-inflammatory and antiproliferative activity against a broad range of human cell lines.<sup>57,59</sup> Our results indicate, however, that these drugs can also inhibit cell growth through the modulation of cholesterol metabolism.

As further evidence of a role for the cholesterol esterification pathway in the growth of pterygium, we demonstrated that the inhibition of cholesterol esterification by SaH and Pg strongly reduced the PF growth rate concomitantly with the loss of cytoplasmic lipids, a pattern similar to that observed with the use of PIO and EVE.

This effect was not caused by cell toxicity because cell morphology and viability were unaffected at the concentrations of inhibitors used. Another interesting finding of this study was that untreated PF expressed higher levels of ACAT1 and MDR1 mRNA than PF treated with cholesterol esterification inhibitors, which instead revealed the presence of very low levels of ACAT1 and MDR1 mRNA.

Whether and how cholesterol esters and proteins involved in the cholesterol ester cycle act in concert to influence cell proliferation remain open questions. A role for cholesterol metabolism during growth is well documented and may be relevant in this context.<sup>57,59</sup> Additionally, a role is reported for MDR1-P-glycoprotein (Pgp) in the transport of several membrane lipids, including the transport of cholesterol from plasma membrane to the ER, the site of cholesterol esterification by ACAT.<sup>21,22,60</sup>

It has been demonstrated that cholesterol esterification depends on the availability of cholesterol, which is transported from the plasma membrane to the ER, and that Pgp encoded by the *MDR1* gene is required for this transport.<sup>61,62</sup>

Caveolae, whose affinity is modified by lipid, particularly free cholesterol, in a site-specific manner in response to physiological stimuli, can be considered specialized platforms for transduction signaling. Studies with cholesterol-depleted cells demonstrated that a reduced level of cholesterol in caveolae is, by itself, a signal to activate pathways leading to cell division.<sup>26,63-66</sup>

Taken together, these findings raise the possibility that MDR-1 might specifically influence caveolae-dependent signaling by regulating, at least in part, the amount of cholesterol available for caveolae formation and that MDR1, cholesterol, and cell proliferation are closely linked.

## CONCLUSIONS AND FUTURE DIRECTIONS

The results of the present study suggest a close functional relationship between cholesterol esterification, *MDR1* gene expression, and rate of cell growth in pterygium. Clearly, the field is expanding, and further research is needed to define the physiological importance of the proposed additional Pgp functions and MDR1. For now, however, we have shown that proteins involved in the cholesterol ester cycle may represent important elements in the control of cell proliferation and of pterygium progression. Furthermore, our data support a potential role for antiproliferation agents such as EVE and PIO as topical medications in the prevention and inhibition of pterygium growth at an early stage,<sup>67</sup> probably by the modulation of cholesterol ester metabolism.

## Acknowledgments

The authors thank Anna Saba and Martina Ciuffo for technical assistance.

## References

1. Sánchez-Thorin JC, Rocha G, Yelin JB. Meta-analysis on the recurrence rates after bare sclera resection with and without mitomycin C use and conjunctival autograft placement in surgery for primary pterygium. *Br J Ophthalmol*. 1998;82:661-665.
2. Hayasaka S, Iwasa Y, Nagaki Y, Kadoi C, Matsumoto M, Hayasaka Y. Late complications after pterygium excision with high dose mitomycin C instillation. *Br J Ophthalmol*. 2000;84:1081-1082.
3. Amano S, Motoyama Y, Oshika T, Eguchi S, Eguchi K. Comparative study of intraoperative mitomycin C and  $\beta$  irradiation in pterygium surgery. *Br J Ophthalmol*. 2000;84:618-621.
4. Hirst LW. The treatment of pterygium. *Surv Ophthalmol*. 2003;48:145-180.
5. Ang LPK, Tan DTH, Cajucom-Uy H, Beuerman RW. Autologous cultivated conjunctival transplantation for pterygium surgery. *Am J Ophthalmol*. 2005;139:611-619.
6. Tosi G-M, Massaro-Giordano M, Caporossi A, Toti P. Amniotic membrane transplantation in ocular surface disorders. *J Cell Physiol*. 2005;202:849-851.
7. Coroneo MT, DiGirolamo N, Wakefield D. The pathogenesis of pterygia. *Curr Opin Ophthalmol*. 1999;10:282-288.
8. Threlfall TJ, English DR. Sun exposure and pterygium of the eye: a dose-response curve. *Am J Ophthalmol*. 1999;128:280-287.
9. Dushku N, John MK, Schultz GS, Reid TW. Pterygia pathogenesis. *Arch Ophthalmol*. 2001;119:695-706.
10. Nolan TM, Di Girolamo N, Sachdev NH, Hampartzoumian T, Coroneo MT, Wakefield D. The role of ultraviolet irradiation and heparin-binding epidermal growth factor-like growth factor in the pathogenesis of pterygium. *Am J Pathol*. 2003;162:567-574.



11. Wlodarczyk J, Whyte P, Cockrum P, Taylor H. Pterygium in Australia: a cost of illness study. *Clin Exp Ophthalmol*. 2001;29:370-375.
12. Clear AS, Chirambo MC, Hutt MSR. Solar keratosis, pterygium and squamous cell carcinoma of the conjunctiva in Malawi. *Br J Ophthalmol*. 1979;63:102-109.
13. Tan DT, Liu YP, Sun L. Flow cytometry measurements of DNA content in primary and recurrent pterygia. *Invest Ophthalmol Visual Sci*. 2000;41:1684-1686.
14. Chan CM, Liu YP, Tan DT. Ocular surface changes in pterygium. *Cornea*. 2002;21:38-42.
15. Chen J-K, Tsai RJF, Lin S-S. Fibroblasts isolated from human pterygia exhibit transformed cell characteristics. *In Vitro Cell Dev Biol*. 1994;30A:243-248.
16. Spandidos DA, Sourvinos G, Kiaris H, Tsamprakakis J. Microsatellite instability and loss of heterozygosity in human pterygia. *Br J Ophthalmol*. 1997;81:493-496.
17. Peiretti E, Dessi S, Mulas MF, Abete C, Galantuomo MS, Fossarello M. Fibroblasts isolated from human pterygia exhibit altered lipid metabolism characteristics. *Exp Eye Res*. 2006;83:536-542.
18. Chuu CP, Hiipakka RA, Kokontis JM, Junichi Fukuchi J, Chen RY, Liao S. Inhibition of tumor growth and progression of LNCaP prostate cancer cells in athymic mice by androgen and liver X receptor agonist. *Cancer Res*. 2006;66:6482-6486.
19. Becker A, Bottcher A, Lackner KJ, et al. Purification, cloning, and expression of a human enzyme with acyl coenzyme A: cholesterol acyltransferase activity, which is identical to liver carboxylesterase. *Arterioscler Thromb Vasc Biol*. 1994;14:1346-1355.
20. Dessi S, Batetta B, Pani A, et al. Role of cholesterol synthesis and esterification in the growth of CEM and MOLT4 lymphoblastic cells. *Biochem J*. 1997;321:603-608.
21. Batetta B, Pani A, Putzolu M, et al. Correlation between cholesterol esterification, MDRI gene expression and rate of cell proliferation in CEM and MOLT4 cell lines. *Cell Prolif*. 1999;32:49-61.
22. Pani A, Batetta B, Putzolu M, et al. MDRI, cholesterol esterification and cell growth: a comparative study in normal and multidrug resistant KB cell lines. *Cell Mol Life Sci*. 2000;57:1094-1103.
23. Ikeda H, Sugiyama Y. Pharmacological effects of a thiazolidinedione derivative, pioglitazone. *Nippon Rinsho*. 2001;59:2191-2194.
24. Schuler W, Sedrani R, Cottens S, et al. SDZ RAD, a new rapamycin derivative: pharmacological properties in vitro and in vivo. *Transplantation*. 1997;64:36-42.
25. Tan DT, Chee SP, Dear KB, Lim AS. Effect of pterygium morphology on pterygium recurrence in a controlled trial comparing conjunctival autografting with bare sclera excision. *Arch Ophthalmol*. 1997;115:1235-1240.
26. Okamoto T, Schlegel A, Scherer PE, Lisanti MP. Caveolins, a family of scaffolding proteins for organizing, "preassembled signal complexes" at the plasma membrane. *J Biol Chem*. 1998;273:5419-5422.
27. Roy S, Luetterforst R, Harding A, et al. Dominant-negative caveolin inhibits H-RAS function by disrupting cholesterol-rich plasma membrane domain. *Nat Cell Biol*. 1999;1:98-105.
28. Dushku N, Reid TW. Immunohistochemical evidence that human pterygia originate from an invasion of vimentin-expressing altered limbal epithelial basal cells. *Curr Eye Res*. 1994;13:473-481.
29. Dushku N, Reid TW. p53 expression in altered limbal basal cells of pingueculae, pterygia, and limbal tumors. *Curr Eye Res*. 1997;16:1179-1192.
30. Tan DT, Lim AS, Goh HS, Smith DR. Abnormal expression of the p53 tumor suppressor gene in the conjunctiva in patients with pterygium. *Am J Ophthalmol*. 1997;123:404-405.
31. Weinstein O, Rosenthal G, Zirkin H, Monos T, Lifshitz T, Argov S. Overexpression of p53 tumor suppressor gene in pterygia. *Eye*. 2002;16:619-621.
32. Tsai YY, Cheng YW, Lee H, Tsai FJ, Tseng SH, Chang KC. p53 gene mutation spectrum and the relationship between gene mutation and protein levels in pterygium. *Mol Vis*. 2005;11:50-55.
33. Shimamura S, Ishioka M, Hanada K, Shimazaki J, Tsubota K. Telomerase activity and p53 expression in pterygia. *Invest Ophthalmol Vis Sci*. 2000;41:1364-1369.
34. Chowers I, Pe'er J, Zamir E, Livni N, Ilisar M, Frucht-Pery J. Proliferative activity and p53 expression in primary and recurrent pterygia. *Ophthalmology*. 2001;108:985-988.
35. Chen PL, Cheng YW, Chiang CC, Tseng SH, Chau PS, Tsai YY. Hypermethylation of the p16 gene promoter in pterygia and its association with the expression of DNA methyltransferase 3b. *Mol Vis*. 2006;12:1411-1416.
36. Fearon E. Tumor-suppressor genes. In: Vogelstein, B, Kinzler KW, eds. *The Genetic Basis of Human Cancer*. New York: McGraw-Hill Health Professional; 1998;229-240.
37. Gallagher MJ, Giannoudis A, Herrington CS, Hiscott P. Human papillomavirus in pterygium. *Br J Ophthalmol*. 2001;85:782-784.
38. Detorakis ET, Sourvinos G, Spandidos DA. Detection of herpes simplex virus and human papilloma virus in ophthalmic pterygium. *Cornea*. 2001;20:164-167.
39. Piras F, Moore PS, Ugalde J, Perra MT, Scarpa A, Sirigu P. Detection of human papillomavirus DNA in pterygia from different geographical regions. *Br J Ophthalmol*. 2003;87:864-866.
40. Kessis TD, Slebos RJ, Nelson WG, et al. Human papillomavirus 16 E6 expression disrupts the p53-mediated cellular response to DNA damage. *Proc Natl Acad Sci USA*. 1993;90:3988-3992.
41. zur Hausen H. Papillomaviruses in human cancer. *Cancer*. 1987;59:1692-1696.
42. Reid TW, Dushku N. Does human papillomavirus cause pterygium? *Br J Ophthalmol*. 2003;87:864-866.
43. Kria L, Ohira A, Amemiya T. Immunohistochemical localization of basic fibroblast growth factor, platelet derived growth factor, transforming growth factor-beta and tumor necrosis factor-alpha in the pterygium. *Acta Histochem*. 1996;98:195-201.
44. Vincenti MP, White LA, Schroen DJ, Benbow U, Brinckerhoff CE. Regulating expression of the gene for matrix metalloproteinase-1 (collagenase): mechanisms that control enzyme activity, transcription, and mRNA stability. *Crit Rev Eukaryot Gene Expr*. 1996;6:391-411.
45. Stetler-Stevenson WG, Liotta LA, Kleiner DE Jr. Extracellular matrix 6: role of matrix metalloproteinases in tumor invasion and metastasis. *FASEB J*. 1993;7:1434-1441.
46. Solomon A, Li DQ, Lee SB, Tseng SC. Regulation of collagenase, stromelysin, and urokinase-type plasminogen activator in primary pterygium body fibroblasts by inflammatory cytokines. *Invest Ophthalmol Vis Sci*. 2000;41:2154-2163.
47. Di Girolamo N, McCluskey P, Lloyd A, Coroneo MT, Wakefield D. Expression of MMPs and TIMPs in human pterygia and cultured pterygium epithelial cells. *Invest Ophthalmol Vis Sci*. 2000;41:671-679.
48. Li DQ, Lee SB, Gunja-Smith Z, et al. Overexpression of collagenase (MMP-1) and stromelysin (MMP-3) by pterygium head fibroblasts. *Arch Ophthalmol*. 2001;119:71-80.
49. Di Girolamo N, Coroneo MT, Wakefield D. UVB-elicited induction of MMP-1 expression in human ocular surface epithelial cells is mediated through the ERK1/2 MAPK-dependent pathway. *Invest Ophthalmol Vis Sci*. 2003;44:4705-4714.
50. Huntington JT, Shields JM, Der CJ, et al. Overexpression of collagenase 1 (MMP-1) is mediated by the ERK pathway in invasive melanoma cells: role of BRAF mutation and fibroblast growth factor signaling. *J Biol Chem*. 2004;279:33168-33176.
51. Perra MT, Colombari R, Maxia C, et al. Finding of conjunctival melanocytic pigmented lesions within pterygium. *Histopathology*. 2006;48:387-393.
52. Solomon A, Grueterich M, Li DQ, Meller D, Lee SB, Tseng SC. Overexpression of insulin-like growth factor-binding protein-2 in pterygium body fibroblasts. *Invest Ophthalmol Vis Sci*. 2003;44:573-580.
53. Kase S, Takahashi S, Sato I, Nakanishi K, Yoshida K, Ohno S. Expression of p27(KIP1) and cyclin D1, and cell proliferation in human pterygium. *Br J Ophthalmol*. 2006 Dec 19 (E-pub ahead of print).
54. John-Aryankalayil M, Dushku N, Jaworski CJ, et al. Microarray and protein analysis of human pterygium. *Mol Vis*. 2006 23;12:55-64.



55. Wong YW, Chew J, Yang H, Tan DT, Beuerman R. Expression of insulin-like growth factor binding protein-3 in pterygium tissue. *Br J Ophthalmol*. 2006;90:769-772.
56. Batteta B, Mulas MF, Sanna F, et al. Role of cholesterol ester pathway in the control of cell cycle in human aortic smooth muscle cells. *FASEB J*. 2003;6:746-748.
57. Dejneka NS, Kuroki AM, Fosnot J, Tang W, Tolentino MJ, Bennett J. Systemic rapamycin inhibits retinal and choroidal neovascularization in mice. *Mol Vis*. 2004;10:964-972.
58. Sarayba MA, Li L, Tungsiripat T, et al. Inhibition of corneal neovascularization by a peroxisome proliferator-activated receptor-gamma ligand. *Exp Eye Res*. 2005;80:435-442.
59. Kwon YS, Kim JC. Inhibition of corneal neovascularization by rapamycin. *Exp Mol Med*. 2006;38:173-179.
60. Batteta B, Mulas MF, Petruzzo P, et al. Opposite pattern of MDR1 and caveolin-1 gene expression in human atherosclerotic lesions and proliferating human smooth muscle cells. *Cell Mol Life Sci*. 2001;58:1113-1120.
61. Metherall JE, Li H, Waugh K. Role of multidrug resistance p-glycoproteins in cholesterol biosynthesis. *J Biol Chem*. 1996;27:2634-2640.
62. Debry P, Nash EA, Neklason DW, Metherall JE. Role of multidrug resistance p-glycoproteins in cholesterol esterification. *J Biol Chem*. 1997;272:1026-1031.
63. Kurzchalia TV, Parton RG. Membrane microdomains and caveolae. *Curr Opin Cell Biol*. 1999;11:424-431.
64. Fielding CJ, Fielding PE. Cholesterol and caveolae: structural and functional relationships. *Biochim Biophys Acta*. 2000;1529:210-222.
65. Simons K, Toomre D. Lipid rafts and signal transduction. *Nat Rev Mol Cell Biol*. 2000;1:31-39.
66. Furuchi T, Anderson RGW. Cholesterol depletion of caveolae causes hyperactivation of extracellular signal-related kinase (ERK). *J Biol Chem*. 1998;273:21099-21104.
67. Solomon AS. Pterygium. *Br J Ophthalmol*. 2006;90:665-666.